Bioorganic & Medicinal Chemistry 21 (2013) 5004–5011

Contents lists available at SciVerse ScienceDirect

Bioorganic & Medicinal Chemistry

journal homepage: www.elsevier.com/locate/bmc

Solid phase synthesis of Smac/DIABLO-derived peptides using a 'Safety-Catch' resin: Identification of potent XIAP BIR3 antagonists

Mohamed A. Elsawy, Lorraine Martin, Irina G. Tikhonova, Brian Walker *

School of Pharmacy, Queen's University of Belfast, 97 Lisburn Road, Belfast BT9 7BL, UK

ARTICLE INFO

Article history:
Received 22 December 2012
Revised 20 June 2013
Accepted 24 June 2013
Available online 2 July 2013

Keywords:
SPPS
Safety-Catch resin
Peptidomimetics
Smac/DIABLO
XIAP BIR3
Cancer resistance
Apoptosis

ABSTRACT

The N-terminal sequence of the Smac/DIABLO protein is known to be involved in binding to the BIR3 domain of the anti-apoptotic proteins IAPs, antagonizing their action. Short peptides and peptide mimetics based on the first 4-residues of Smac/DIABLO have been demonstrated to re-sensitize resistant cancer cells, over-expressing IAPs, to apoptosis. Based on the well-defined structural basis for this interaction, a small focused library of C-terminal capped Smac/DIABLO-derived peptides was designed in silico using docking to the XIAP BIR3 domain. The top-ranked computational hits were conveniently synthesized employing Solid Phase Synthesis (SPS) on an alkane sulfonamide 'Safety-Catch' resin. This novel approach afforded the rapid synthesis of the target peptide library with high flexibility for the introduction of various C-terminal amide-capping groups. The library members were obtained in high yield (>65%) and purity (>85%), upon nucleophilic release from the activated resin by treatment with various amine nucleophiles. In vitro caspase-9 activity reconstitution assays of the peptides in the presence of the recombinant BIR3-domain of human XIAP (500 nM) revealed *N*-methylalanyl-tertiarybutylglycinyl-4-(*R*)-phenoxyprolyl-*N*-biphenylmethyl carboxamide (**11a**) to be the most potent XIAP BIR3 antagonist of the series synthesized inducing 93% recovery of caspase-9 activity, when used at 1 μM concentration. Compound (**11a**) also demonstrated moderate cytotoxicity against the breast cancer cell lines MDA-MB-231 and MCF-7, compared to the Smac/DIABLO-derived wild-type peptide sequences that were totally inactive in the same cell lines.

1. Introduction

The ability of cancer cells to suppress apoptosis induced by conventional chemotherapeutic agents is achieved by the up-regulation of various anti-apoptotic proteins. The Inhibitor of Apoptosis Proteins (IAPs) constitute one such family of anti-apoptotic proteins that are over-expressed in many tumours and which inhibit caspase activation,[1–9] making those tumours intensively impervious to traditional chemotherapeutics and radiotherapy. X-linked IAP (XIAP) exhibits the most pronounced anti-apoptotic effect among the IAP family.[3–10] XIAP inhibits the apoptosome-mediated activation of the initiator caspase, caspase-9, through binding to the protease via its third Baculovirus IAP Repeat (BIR3) domain and sequestering it in an inactive monomeric form.

Recently, a pro-apoptotic mitochondrial protein; Second mitochondria-derived activator of caspases (Smac), known also as Direct IAP Binding protein with LOw pI (DIABLO), was discovered to bind to and inhibit IAPs at the BIR3 domain, relieving capases from their inhibition and thus permitting the re-activation of the apoptosis machinery.[5,6] Interestingly, many studies have demonstrated that only the N-terminal residues of Smac/DIABLO are essential for its pro-apoptotic function.[11–14] Moreover, other studies showed that the Smac/DIABLO-derived N-terminal short peptides conjugated to cell penetrating carrier peptides are able to overcome the XIAP-mediated apoptosis resistance, and re-sensitized cancer cells, over-expressing XIAP, to various anticancer drugs both in vitro and in vivo.[15–17] Also, those peptides exhibited a low toxicity profile in normal cells, which make them potentially highly selective anticancer agents.

These attributes pinpoint the Smac/DIABLO-derived peptides as potential anti-cancer therapeutic agents, though their entirely peptidic nature may limit their therapeutic utilization. This is because of the intrinsic and generally poor bioavailability of peptides owing to their inability to penetrate cell membranes and instability towards proteolytic cleavage. Consequently, many research groups have focused on developing peptidomimetic[18–21] and non-peptidic[22,23] Smac/DIABLO mimics, in attempts to generate XIAP BIR3 tight-binders with improved bioavailability.

In this paper, we report on a new Solid Phase Synthesis (SPS) strategy for the generation of novel Smac/DIABLO-derived peptides using a 'Safety-Catch' resin. This strategy represents an original approach for the facile expedited synthesis of such peptides that were previously only available through classical solution methods,

* Corresponding author. Tel.: +44 2890972117; fax: +44 2890977794.
E-mail address: brian.walker@qub.ac.uk (B. Walker).

0968-0896/$ - see front matter © 2013 Elsevier Ltd. All rights reserved.
http://dx.doi.org/10.1016/j.bmc.2013.06.055

which are more time consuming. The approach has been utilized for the preparation of XIAP BIR3 antagonist sequences identified using in silico structure-guided design. The peptides produced have been shown to be potent XIAP BIR3 inhibitors in caspase-9 reactivation assays and demonstrated moderate cytotoxicity in cellular context compared to the totally inactive Smac/DIABLO-derived wild type sequences.

2. Materials and methods

2.1. Synthesis

All amino acids were introduced as their Fmoc protected derivatives. Fmoc-Ala-OH, Fmoc-Phe-OH and Fmoc-Pro-OH were purchased from CEM (Buckingham, England, UK). 4-Sulfamylbutyryl AM 'Safety-Catch' resin (substitution 0.8 mmol/g), Fmoc-Tic-OH, Fmoc-Tyr-(*t*Bu)-OH and Fmoc-Val-OH were obtained from Novabiochem (Darmstadt, Germany). Fmoc-*N*-Me-Ala-OH and Fmoc-Tle-OH were supplied by BACHEM (Weil am Rhein, Germany). (2*S*,4*R*)-Fmoc-4-phenyl-pyrrolidine-2-carboxylic acid and (2*S*,4*S*)-Fmoc-4-phenoxy-pyrrolidine-2-carboxylic acid were purchased from PolyPeptide Group (Strasbourg, France). Benzotriazole-1-yl-oxy-tris-pyrrolidino-phosphonium hexafluorophosphate (PyBop), *O*-(benzotriazol-1-yl)-*N*,*N*,*N*′,*N*′-tetramethyluronium hexafluorophosphate (HBTU) and Rink amide MBHA resin (substitution 0.65 mmol/g, 100–200 mesh) were obtained from Iris Biotech GMBH (Marktredwitz, Germany). Anhydrous magnesium sulfate, benzhydrylamine, carbonyldiimidazole, dichloromethane (CH_2Cl_2), diethylether, diisopropylethylamine (DIEA), HPLC grade methanol, HPLC grade trifluoroacetic acid, HPLC grade water, iodoacetonitrile, Kaiser Test Kit, 1-methyl-2-pyrrolidone (NMP), *N*,*N*-dimethylformamide (DMF), piperidine, (*R*)-(−)-1,2,3,4-tetrahydro-1-naphthylamine, tetrahydrofuran (THF), trifluoroacetic acid (TFA) and triisopropylsilane were all obtained from Sigma–Aldrich (Gillingham, Dorset, England, UK). C-(1*H*-Indol-3-yl)-methylamine was purchased from Rare Chemicals GmbH (Kiel, Germany). Doubly distilled, deionised water was used throughout (17–18 mΩ).

2.1.1. Protocol for the microwave assisted solid phase peptide synthesis (MW-SPPS) for sequence assembly

Peptides were synthesized on a CEM Liberty™ automated microwave peptide synthesizer (CEM Microwave Technology Ltd, Buckingham, England, UK). In essence, each peptide was synthesised, on a 0.1–0.5 mmol scale, using either Rink Amide MBHA resin (substitution 0.65 mmol/g, 100–200 mesh) for peptides (**18**–**20**) or a pre-loaded 4-Sulfamylbutyryl AM resin (substitution 0.6–0.8 mmol/g, loaded as described under Section 2.1.2) for peptides (**10a**) and (**11a**–**f**). Fmoc removal was performed using 2 repeat cycles employing 20% (V/V) piperidine as solution in DMF. A first deprotection cycle of 30 s at 50 W was employed, followed by a second deprotection cycle of 3 min at 50 W. Both cycles were carried out at 75 °C. Coupling steps were carried out by introducing each Fmoc-amino acid (0.2 M solution in DMF) at a fivefold excess over resin loading, together with HBTU activation reagent and DIEA activation base used in the molar ratios HBTU/DIEA/AA (1/2/1). Each coupling reaction was performed for 10 min, at 22 W, at 75 °C. Finally, cleavage of peptides (**18**–**20**) from Rink Amide MBHA was performed manually, at room temperature, using TFA/H_2O/triisopropylsilane (95/2.5/2.5, v/v/v), for two 1 h cycles, with washing with dichloromethane after every cycle. The collected cleavage reaction mixtures and washes were evaporated under vacuum, at 30 °C, cooled, and the products precipitated by the addition of cold diethylether. The precipitates were collected by centrifugation (3–5 min at 2000–3000*g*) and the pellet washed thoroughly with diethylether. This process was repeated 2–3 times, each time the solid was collected by centrifugation. On the other hand, cleavage of peptides **10a** and **11a**–**f** from 4-Sulfamylbutyryl AM resin was performed as described under Section 2.1.3. After a brief drying in vacuum to remove all traces of solvents, the peptide products were dissolved in 10% TFA aqueous solution and freeze dried. Peptide purity was checked through RP-HPLC, using Waters HPLC system fitted with Waters 1525 binary HPLC pump and Waters 2489 UV/visible detector (λ_{216} nm) (Waters, Milford, Massachusetts, USA) and employing a Phenomenex Jupiter C12 column (250 × 4.66 mm; particle size, 10 μm). The runs were carried out on an analytical scale with a flow rate of 1 ml/min. An elution gradient was utilized to resolve the crude product components that went from 90% solvent A (0.05% TFA in H_2O)/10% Solvent B (0.05% TFA in CH_3OH) to 10% solvent A/90% solvent B in 60 min. Peptides with crude purity less than 95% were purified with semi-preparative RP-HPLC, using Phenomenex Jupiter C12 column (250 × 21.20 mm; particle size, 10 μm) and using the same above stated elution gradient with a flow rate of 10 ml/min.

2.1.2. General procedure for 4-sulfamylbutyryl AM 'Safety-Catch' resin loading

4-Sulfamylbutyryl AM Resin (625 mg, 0.5 mmol) suspended in 17 ml $CHCl_3$, DIEA (476.6 μl, 2.5 mmol) and an Fmoc-amino acid [(2*S*,4*R*)-Fmoc-4-phenyl-pyrrolidine-2-carboxylic acid (620 mg, 1.5 mmol); (2*S*,4*S*)-Fmoc-4-phenoxy-pyrrolidine-2-carboxylic acid (643 mg, 1.5 mmol); Fmoc-Tic-OH (600 mg, 1.5 mmol)] were added to a 100 ml round bottom flask. The reaction mixture was stirred for 10 min, cooled to −20 °C and after 20 min PyBop (780 mg, 1.5 mmol) was added as solid. The reaction mixture was stirred for 8 h at −20 °C after which the resin was filtered and washed with $CHCl_3$ (3 × 5 ml). The resin was dried in a desiccator under vacuum. The resin loading was checked spectrophotometrically by performing Fmoc-group removal on accurately weighed samples (~4 mg) of resin derivatized by these three Fmoc-derivatives, and measuring the formation of the dibenzofulvene-piperidine adduct (molar absorptivity $\varepsilon = 5253\ M^{-1}\ cm^{-1}$ at λ_{290} nm), using a UV spectrophotometer (50 Scan UV–Visible Spectrophotometer, VARIAN, Australia).

2.1.3. Peptide cleavage from 4-sulfamylbutyryl AM 'Safety-Catch' resin

After peptide assembly on the 4-sulfamylbutyryl AM Resin, the resin was activated by iodoacetonitrile to produce a resin-bound *N*,*N*-cyanomethylacylsulfonamide (**8**, **9a**–**b**). In the activation procedure, the resin (0.5 mmol) was washed several times with NMP, followed by the addition of 8 ml NMP and DIEA (480 μl, 2.5 mmol) to the swollen resin. Then, iodoacetonitrile (734 μl, 10 mmol) was added to the reaction mixture, which was protected from direct exposure to light. The reaction mixture was stirred for 24 h, filtered and washed with NMP (5 × 5 ml, >10 min/wash), CH_2Cl_2 (3 × 5 ml). The resin was then suspended in 15 ml THF and transferred to 100 ml round bottom flask, to which the corresponding primary amine was added [benzhydrylamine (458 mg, 2.5 mmol); (*R*)-(−)-1,2,3,4-tetrahydro-1-naphthylamine (368 mg, 2.5 mmol); C-(1*H*-Indol-3-yl)-methylamine (364 mg, 2.5 mmol)]. The reaction mixture was stirred for 4 h, filtered and washed with THF several times. The combined filtrate and washes were evaporated under vacuum, at 30 °C, dissolved in water and freeze dried.

2.2. Structural modeling

Automated docking was conducted with GLIDE 5.6 of Schrödinger suite 9.0 using the Extra Precision XP algorithm.[24,25] The crystal structure of the BIR3 domain of XIAP with the PDB code 1G3F, was refined with the Protein Preparation module of Schrödinger suite 9.0 and used for the docking studies. The binding site was defined as the residues located within 6 Å from the ligand. To

compensate for the rigid representation of the receptor, the Van der Waals radii of the atoms were scaled by factor 0.65 to generate the receptor grid. All compounds were pre-processed with LigPrep 2.4 of Schrödinger at pH 7. Default settings were used for the docking protocol. The final ligand poses were selected based on the GLIDE empirical docking scores (GlideScore) and the overall complementary to the binding cavity identified visually. The OPLS2005 force field was used for all calculations.

2.3. In vitro assays

Cytochrome c from bovine heart, 2′-deoxyadenosine 5′-triphosphate disodium salt (dATP), dimethylsulphoxide (DMSO), 3-[4,5-dimethylthiazol-2-yl]-2,5-diphenyltetrazolium bromide (MTT) Human recombinant Dipeptidyl Peptidase IV (DPP-IV) enzyme expressed in SF9 cells, microsomal Leucine Aminopeptidase (LAP) enzyme type IV-S from porcine kidney microsomes, tris(hydroxymethyl)aminomethane (Trizma® base), sodium chloride (NaCl) and potassium chloride (KCl) were obtained from Sigma–Aldrich Chemical Company (Gillingham, Dorset, England, UK). Caspase-9 Fluorimetric Assay Assay Kit (BioVision) was purchased from Enzo® Life Sciences, Exeter, UK). The kit contained lysis buffer, assay buffer and LEHD-AFC substrate. A Protease inhibitor cocktail was prepared from a proteases inhibitor set obtained from Roche Applied Sciences (West Sussex, England, UK). Recombinant Human XIAP BIR3 Domain (rhXIAP BIR3) was supplied by R&D systems® (Abingdon, Oxfordshire, England, UK). Doubly distilled, deionised water was used for buffers preparation (17–18 m Ω).

2.3.1. Caspase-9 activity fluorimetric assay

MDA-MB-231 cell lysates were prepared by solubilising cell pellets (~5×10^7 cells) in 1 ml ice cold lysis buffer (50 mM KCl, 5 mM EGTA, 2 mM $MgCl_2$, 1 mM DTT, 0.2% CHAPS and 50 mM HEPES; pH 7.4), supplemented with a protease inhibitor cocktail (50 μg/ml Antipain. 2HCl, 40 μg/ml Bestatin, 6 μg/ml Chymostatin, 7 μg/ml Pepstatin, 50 μg/ml Phosphoramidon, 1 mg/ml Pefabloc SC, 0.5 mg/ml EDTA-Na_2 and 2 μg/ml Aprotinin), and stored on ice prior to their use (<30 min). 5 μl of Cytochrome c (1 mg/ml) and dATP (5 mM) in assay buffer (10 mM HEPES, 0.5 mM EGTA, 5 mM DTT and 10% Glycerol; pH 7.4) were added to 25 μl of cell lysate contained in a 1.5 ml microcentrifuge tube. To this was added 1 μl rhXIAP BIR3 (500 nM final concentration) and 0.5 μl peptide treatment in DMSO (final concentrations of 1 μM, 0.1 μM and 0.01 μM), which were then incubated, at 37 °C, for 1 h. Controls were set up in which recombinant XIAP BIR3 domain and/or peptide treatments were replaced with the vehicles used to dissolve each, as appropriate. Each treatment/control was then diluted with 65 μl of assay buffer, transferred to individual wells of a 96-well microtiter plate, and 5 μl of a solution of the fluorogenic substrate Ac-LEHD-AFC (in DMF) was then added to each well, to give a final substrate concentration of 50 μM. Caspase-9 activity in each sample well was then monitored (λ_{ex} 380–400; λ_{em} 470–500) by following the increase in fluorescence due to the formation of 7-amino-4-trifluoromethylcoumarin from the hydrolysis of Ac-LEHD-AFC, catalysed by the protease, using a FLUOstar OPTIMA spectrofluorimeter (BMG LABTECH, Ortenberg, Germany). Caspase-9 activity was monitored for 1 h, at 37 °C. Reactions were carried out in duplicate. Finally, the % caspase-9 'relief' was calculated by relating the rate of hydrolysis of the fluorogenic substrate in the presence of 1 μM peptide +500 nM rhXIAP BIR3 to the maximum rate obtained in the absence of the recombinant protein, in lysates treated with cytochrome C and dATP according to the following formula:

$$\%\ \text{Caspase 9relief} = 100 \times [\text{slop of treatment curve fit}/\text{slop of maximum activation (dATP + cyt.c) curve fit}]$$

2.3.2. Cell viability assays (MTT assays)

Cells were seeded onto sterile 96-well culture plates at densities of 1×10^4 cells/well for MDA-MB-231 cells and 2×10^4 cells/well for MCF-7 cells. Cells were incubated, for 24 h, at 37 °C and 5% CO_2, after which media was aspirated from cells and 100 μl fresh media with/without treatments were added. Control wells were treated with media containing the DMSO vehicle at concentrations equivalent to those used in the peptide treatments. Cells were further incubated at 37 °C and 5% CO_2 for 72 h, followed by the addition of MTT (10 μl of a 10 mg/ml solution) to each well. Following 2 h incubation of the plate at 37 °C and 5% CO_2 and shielded from light with tin foil, the media was removed and the produced formazan crystals were solubilised by the addition of 200 μl of DMSO. Colour intensity was measured quantitatively at 550 nm using an EL808 HiTeck™ Spectra Thermo plate reader (HiTeck Instruments, USA).

3. Results and discussion

3.1. Synthesis

A library of new Smac/DIABLO-derived peptidomimetics (Table 1) was designed and selected for synthesis on the basis of the in silico study performed as a part of the present investigation (see Section 3.2), which was guided/informed by the well defined structural information for the binding of Smac/DIABLO analogues to XIAP BIR3.[13,14]

A novel SPS strategy for the efficient preparation of the target library was adapted, based on the use of an alkane-sulfonamide 'Safety-Catch' resin, first introduced by Backes and Ellman.[26] The feature of resins with a safety-catch linker is that the peptide product cannot be released by treatment with TFA and thus these resins are suitable for both Fmoc- and Boc-SPPS. Rather, product cleavage from such resins can be accomplished by a two-step process that requires activation of the linker followed by reaction with a nucleophile.[26–28] This is most usually achieved by alkylation of the sulfonamide linker by an electrophilic halide (activation step), followed by cleavage with a nucleophile, which in the present study was an aryl–alkyl amine so as to produce the target C-terminal capped peptide amides. This synthetic strategy was deemed attractive for the synthesis of the target library, since it affords high flexibility for the introduction of various C-terminal capping groups by releasing the resin-tethered tripeptide sequences [*N*-Me-Ala-Tle-X-Resin, where X is either Tic (**6**) or 4-substituted Pro (**7a**,**b**)] with different amine nucleophiles (Scheme 1).

The 'Safety-Catch' 4-sulfamylbutyryl AM resin was first loaded with either Fmoc-Tic-OH (**2**) or 4-substituted Fmoc-Pro-OH (**3a** or **3b**). The loading was carried out, conventionally, for 8 h, at −20 °C, in $CHCl_3$ using PyBop as an activator and DIEA as an activator base. The % resin loading achieved was 86% (0.69 mmol/g) for (**2**), 81% (0.65 mmol/g) for (**3a**) and 90% (0.72 mmol/g) for (**3b**), as determined spectrophotometrically. After confirming successful resin loading, the target sequences were then extended by incorporation of Fmoc-Tle-OH and Fmoc-*N*-Me-Ala-OH, through brief cycles of MW-assisted SPS.

As mentioned above, peptide release from the resin requires pre-activation of the 'Safety-Catch' linker by reaction with various electrophiles. We employed the frequently used iodoacetonitrile as the activator electrophile. The activated peptide-safety-catch resins (**8**, **9a**–**b**) were then treated with a range of aryl–alkyl amines to produce the library of C-terminal capped Smac/DIABLO-derived peptidomimetics listed in Table 1. As can be appreciated from this table, the purity and yields of the crude products (**11a**–**d**) are relatively high (>85%, see Table 1 and Supplementary Figs. S1 and S2). In comparison, the crude compounds (**10a**) and (**11e**,**f**) were obtained in low yields and purity. We suspect that the reason for

Table 1
Library of Smac/DIABLO-derived peptidomimetics synthesized in the present study

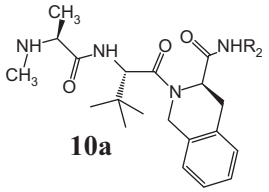

10a

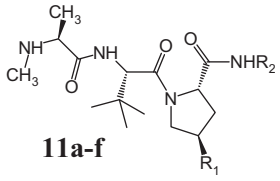

11a-f

Compound no.	R_1	R_2	Purity[a] (%)	RT (min)	Yield (%)	TOF-MS[b]		^{1}H NMR (DMSO-d_6, 400 MHz), δ ppm
						Calculated	Found	
10a	NA[c]	Indolyl-3-methyl	45	31	28	503.2918	503.2909	0.879 (s, 9H), 1.228 (d, 3H), 2.83 (d, 2H), 3.298–3.679 (m, 3H), 3.85 (m, 1H), 4.13 (m, 1H), 4.34–4.68 (m, 3H), 6.78–7.04 (m, 6H), 7.36–7.44 (m, 2H)
11a	C_6H_5O	$(C_6H_5)_2CH$	99	28	85	570.3261	570.3284	0.91 (s, 9H), 1.296 (d, 3H), 2.327 (m, 2H), 2.46 (s, 3H), 3.65 (d, 2H), 4.08 (m, 1H), 4.21 (m, 1H), 4.73 (m, 1H), 6.28 (s, 1H), 6.98–7.12 (d, 6H), 7.23–7.45 (m, 9H)
11b	C_6H_5	(*R*)-1-Tetrahydronaphthyl	98	18	87	535.3284	535.3298	0.876 (s, 9H), 1.278 (d, 3H), 1.243–1.349 (m, 4H), 2.39 (m, 2H), 2.52–2.75 (m, 2H), 3.34–3.82 (m, 3H), 4.12 (m, 1H), 4.34 (s, 1H), 4.62 (m, 1H), 7.16–7.18 (m, 3H), 7.25–7.48 (m, 6H)
11c	C_6H_5	$(C_6H_5)_2CH$	95	26	76	555.3335	555.3336	0.857 (s, 9H), 1.316 (d, 3H), 2.27 (m, 2H), 2.43 (s, 3H), 3.38 (m, 1H), 3.62 (d, 2H), 3.98 (m, 1H), 4.18 (m, 1H), 6.37 (s, 1H), 7.06–7.14 (d, 6H), 7.28–7.48 (m, 9H)
11d	C_6H_5	(*R*)-1-Tetrahydronaphthyl	85	15	64	519.3335	519.3337	0.86 (s, 9H), 1.28 (d, 3H), 1.58 (d, 2H), 1.77–1.94 (m, 2H), 2.20 (m, 2H), 2.65–2.73 (m, 2H), 3.29 (m, 1H), 3.58–3.78 (m, 3H), 4.16 (m, 1H), 6.92–7.09 (m, 3H), 7.29–7.43 (m, 6H)
11e	C_6H_5O	Indolyl-3-methyl	35	27	18	551.3426	551.3411	0.995 (s, 9H), 1.24 (d, 3H), 2.31 (m, 2H), 3.34 (m, 1H), 3.62–3.85 (m, 6H), 4.18–4.2 (m, 3H), 6.83–7.09 (m, 6H), 7.27–7.39 (m, 3H)
11f	C_6H_5	Indolyl-3-methyl	32	28	13	535.3437	535.3456	0.91 (s, 9H), 1.25 (d, 3H), 2.1 (m, 2H), 3.28 (m, 1H), 3.46–3.62 (m, 6H), 4.11 (s, 1H), 4.14 (s, 1H), 6.88–6.94 (m, 4H), 7.27–7.39 (m, 5H)

[a] % Purity of the crude product as estimated from its RP-HPLC chromatogram.
[b] TOF-MS, Time of Flight-Mass Spectrometry.
[c] NA, not applicable.

this is that the Indol-3-yl methylamine, which is the common amine nucleophile used for release and C-terminal capping of the three products, was sourced commercially and was found to be of dubious quality, and is likely to be the reason behind the low purity profile for those compounds.

3.2. In silico studies and in vitro assays

The structural basis for the interaction of the short N-terminal segment of Smac/DIABLO with XIAP BIR3 domain is well defined.[13,14] The structure of the Smac/DIABLO-XIAP BIR3 complex (PDB code: 1G3F) shows that the Smac/DIABLO N-terminal tetrapeptide sequence AVPI possesses an extended conformation along the third β-strand of the XIAP BIR3 domain and has identified specific inter-molecular interactions that appear to be crucial for complex stability (Fig. 1). For example, possible electrostatic interaction between the Smac/DIABLO peptide N-terminal amino group and the proximal carboxylate of E314 in XIAP BIR3 seem likely to occur. Also, the side-chain methyl group of Ala is accommodated into a hydrophobic pocket formed by the W310 residue of the protein, in which it most likely interacts with the indole ring of the tryptophan residue. As can also by appreciated from Figure 1, the isopropyl side chain of the P2 Val residue of Smac is protruding outside the XIAP BIR3 binding pocket and is solvent exposed, which reflects its minor role in the interaction. At P3, the Smac/DIABLO main chain amide backbone is slightly twisted, due to the presence of a proline residue at this position. It can be appreciated that the orientation of the proline residue could possibly favour hydrophobic interactions between the gamma (position-4) and delta (position-5) methylene groups of the pyrrolidine ring with the indole ring of W323 (Fig. 1). It can also be observed from Figure 1 that there is a deep hydrophobic pocket formed by the residues W323 and Y324 that can accommodate an extra aromatic substituent at the gamma (4) position of the proline residue. Another hydrophobic channel formed between the aliphatic hydrocarbon side-chains of residues K297 and K299 ($-[CH_2]_4-$) accommodates the Ile residue at the P4 position of Smac/DIABLO (Fig. 1). This suggested to us that an aromatic ring could possibly be slotted between these two residues so as to improve/enhance the binding affinity of Smac/DIABLO-derived molecule to XIAP BIR3.

Based on this analysis of the structure of the complex, we constructed two libraries in silico. The first library comprised molecules in which the nature of the R_1 substituent at the 4-position of the P3 proline residue was varied, along with the aromatic C-terminal amide capping group (R_2) to give the general structures (**11a**–**s**), shown below (Table 2 and Supplementary Table S3), which includes the peptide *N*-methylalanyl-tertiarybutylglycinyl-4-(*S*)-phenoxyprolyl-*N*-(*R*)-1-tetrahydronaphthyl carboxamide (**11g**), previously reported to be a potent antagonist of rhXIAP BIR3 (**Table 2**).[18] In the secondlibrary, the P3 Pro residue was replaced by tetrahydroisoquinoline carboxylate (Tic). Tic is also an amino acid and can be considered as a highly constrained analogue of 4-phenyl-proline. Once again, the aromatic C-terminal capping group (R_2) of the Tic-containing peptide was varied to give the general structures (**10a**–**c**) (Table 2 and Supplementary Table S3). High-throughput docking of the 22 virtual ligands into the XIAP BIR3 binding site was carried out using GLIDE (Schrödinger), employing the GlideScore scoring function.[24,25] The docking scores for the best fitting ligands are shown in Table 2. On the other hand, in silicocompounds (**10b**,**c**) and (**11h**–**s**) were not accommodated in the XIAP BIR3 pocket (see Supplementary Table S3 for precise structures), which is most likely due to their steric bulk. Consequently, it was decided not to synthesize and test these examples.

The overlay of some of the analogues prepared in the present study (shown in yellow) with the Smac/DIABLO-derived

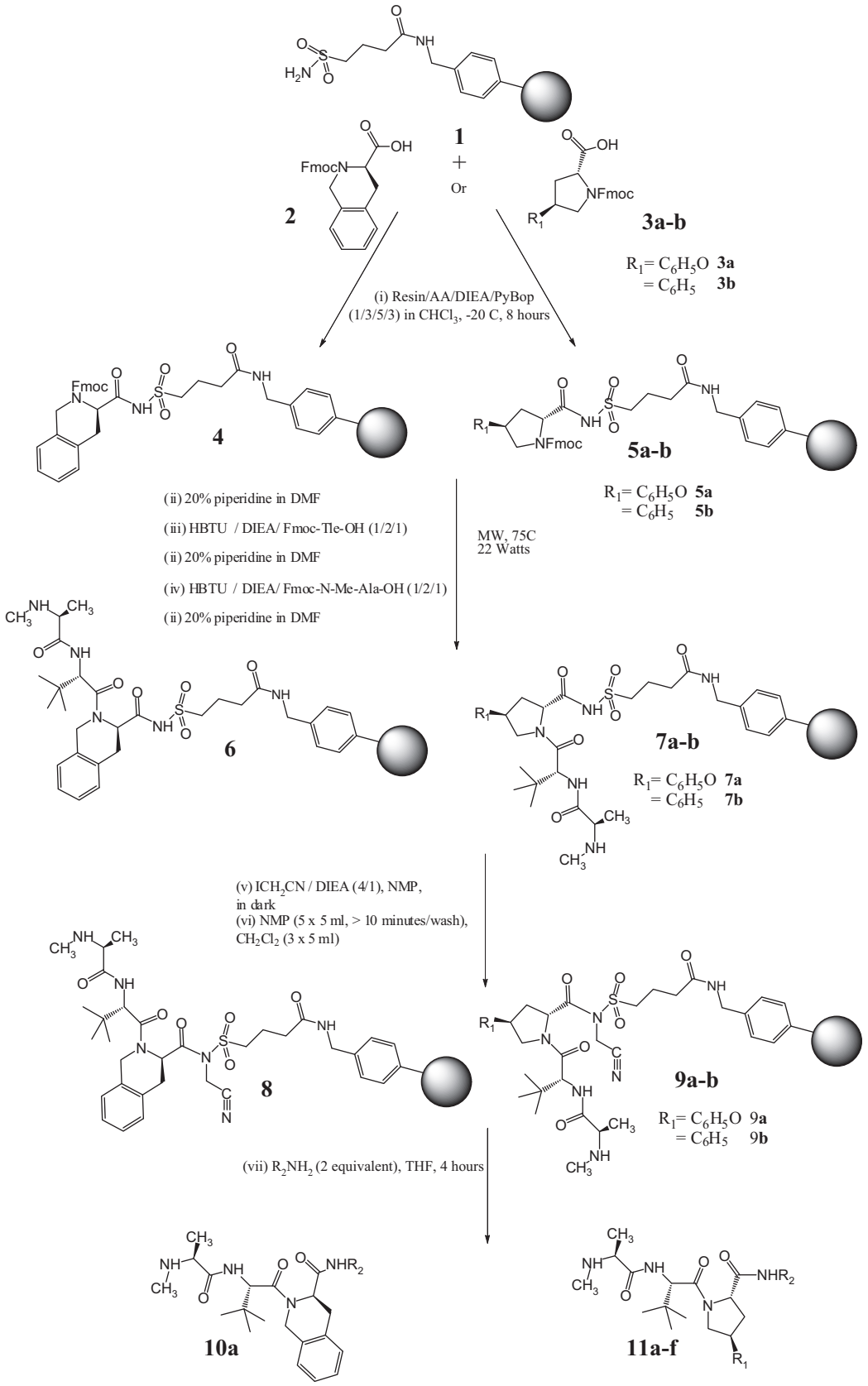

Scheme 1. Scheme for the synthesis of Smac/DIABLO-derived peptidomimetics showing loading of the first amino acid onto and release of product by aminolysis from 4-sulfamylbutyryl AM 'Safety-Catch' resin.

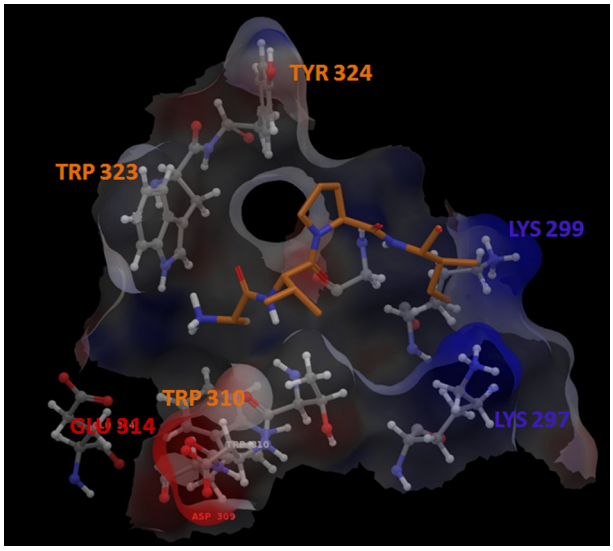

Figure 1. Smac/DIABLO-derived N-terminal sequence AVPI (orange) in the XIAP BIR3 binding pocket; generated from PDB: 1G3F.[13] Only residues forming the direct contacts with the peptide are visualized and the shape of the binding cavity are shown with the surface-like representation coloured based on the location of the negative and positive charge residues.

peptidomimetic (**11g**) (shown in green) within the XIAP BIR3 binding site are shown in Figure 2, where (**11g**) is to our knowledge the tightest reported binder to XIAP BIR3 (K_d = 5 nM, Oost et al.[18]) It is obvious from Figure 2a, that (**11b**) is one of the best overlapping matching candidates with peptidomimetic (**11g**). The in silico docking score of (**11b**) was −7.05 Kcal/mol compared to only −3.81 Kcal/mol for its enantiomer (**11g**) (Table 2 and Fig. 2a). The differences in docking score could be attributable to the 'inversion' of the configuration of the 4-phenoxy group from *S* in (**11g**) to *R* in (**11b**). This inversion would serve to position/place the phenyl ring deeper into the hydrophobic pocket formed by residues W323 and Y324, which could lead to additional π–π interactions between the 4-(*R*)-phenoxy phenyl ring of the peptide with the aromatic side-chains of both residues (Fig. 2a). This would be possible because of the rotation of the phenyl ring of the 4-(*R*)-phenoxy grouping about the C–O ether bond, thus permitting interaction with both W323 and Y324 residues. The replacement of the 4-(*R*)-phenoxy with the more rigid 4-(*S*)-phenyl group at P3 does not seem to make a big difference in the docking score of (**11c**) compared to its phenoxy analogue (**11a**) (Table 2). However, there is an appreciable drop in the docking score of the 4-(*S*)-phenyl substituted analogues (**11d**) and (**11f**) when compared to their 4-(*R*)-phenoxy congeners (**11b**) and (**11e**) (Table 2 and Fig. 2b). Finally, no significant differences in the docking scores were observed as a result of varying the C-terminal aromatic capping between tetrahydronaphthyl, indolyl and biphenyl groups with the exception of the best fitting candidate (**11b**) (Table 2). On the other hand, (**10a**) was accommodated particularly readily, with the Tic tetrahydroisoquinoline fused ring of this analogue overlapping with the 4-(*S*)-phenoxy-substituted proline residue of the previously reported analogue (**11g**). This predicted accommodation of (**10a**), preserves the hydrophobic interaction with W323 (data not shown).

The top-ranked hits based on the GlideScore function and the pocket fitting were conveniently synthesized as described in Section 3.1 above and tested for their XIAP BIR3 inhibitory activity through a caspase-9 activity reconstitution assay. In this assay, the ability of the Smac/DIABLO-derived analogue to recover caspase-9 activity in the presence of 500 nM rhXIAP BIR3 was determined by the % increase in caspase-9 activity that they promoted.

The XIAP BIR3 inhibition observed for the 4-(*R*)-phenoxy substituted compounds (**11a**), (**11b**) and (**11e**) of % caspase-9 relief 93.1 ± 7.9, 87.6 ± 6.2 and 64.9 ± 9.3 is slightly-but not significantly-higher than that caused by their 4-(*S*)-phenyl analogues (**11c**), (**11d**) and (**11f**) of % caspase-9 relief 89.4 ± 5.8, 83.7 ± 7.1 and 61.6 ± 8.6, respectively (Table 2 and Fig. 3). Also, the XIAP BIR3 inhibition was slightly-but not significantly-improved when the tetrahydronaphthyl amide C-terminal capping group of analogues (**11b**) and (**11d**) of % caspase-9 relief 87.6 ± 6.2 and 83.7 ± 7.1 was replaced with the biphenyl amide group in analogues (**11a**) and (**11c**) of % caspase-9 relief 93.1 ± 7.9 and 89.4 ± 5.8, respectively (Table 2). On the other hand, the C-terminal capping with an indanylmethyl amide group caused ~1.4-fold significant reduction in the XIAP BIR3 inhibitory activity of (**11e**) and (**11f**) of % caspase-9 relief 64.9 ± 9.3 and 61.6 ± 8.6, respectively, when compared to their biphenyl amide analogues (**11a**) and (**11c**) of % caspase-9 relief 93.1 ± 7.9 and 89.4 ± 5.8, respectively,

Table 2
Smac-derived peptidomimetic libraries docking scores and bioassays data

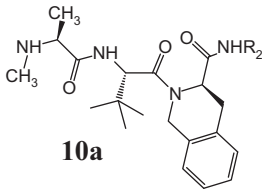

10a

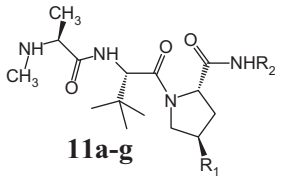

11a-g

Compound. no.	R_1	R_2	Glide docking score (Kcal/mol)	% Caspase-9 relief[a]	% Viability[b]	
					MDA-MB-231	MCF-7
10a	Not applicable	Indolyl-3-methyl	−4.598	66.3 ± 8.4	ND[c]	ND
11a	(*R*)-C_6H_5O	$(C_6H_5)_2CH$	−5.045	93.1 ± 7.9	50.3 ± 7.9	58.6 ± 9.7
11b	(*R*)-C_6H_5O	(*R*)-1-Tetrahydronaphthyl	−7.05	87.6 ± 6.2	58.1 ± 7.2	70.8 ± 11.2
11c	(*S*)-C_6H_5	$(C_6H_5)_2CH$	−5.409	89.4 ± 5.8	50.1 ± 6.5	62.3 ± 7.9
11d	(*S*)-C_6H_5	(*R*)-1-Tetrahydronaphthyl	−4.68	83.7 ± 7.1	54.6 ± 11.9	79.4 ± 12.3
11e	(*R*)-C_6H_5O	Indolyl-3-methyl	−6.447	64.9 ± 9.3	ND	ND
11f	(*S*)-C_6H_5	Indolyl-3-methyl	−4.215	61.6 ± 8.6	ND	ND
11g[d]	(*S*)-C_6H_5O	(*R*)-1-Tetrahydronaphthyl	−3.81	NA	NA	NA

[a] Treatments were used at 1 μM concentration.
[b] % Viability at 100 μM concentration.
[c] NA, data not available; ND, not determined.
[d] K_d = 5 nM, as reported by Oost et al.[18]

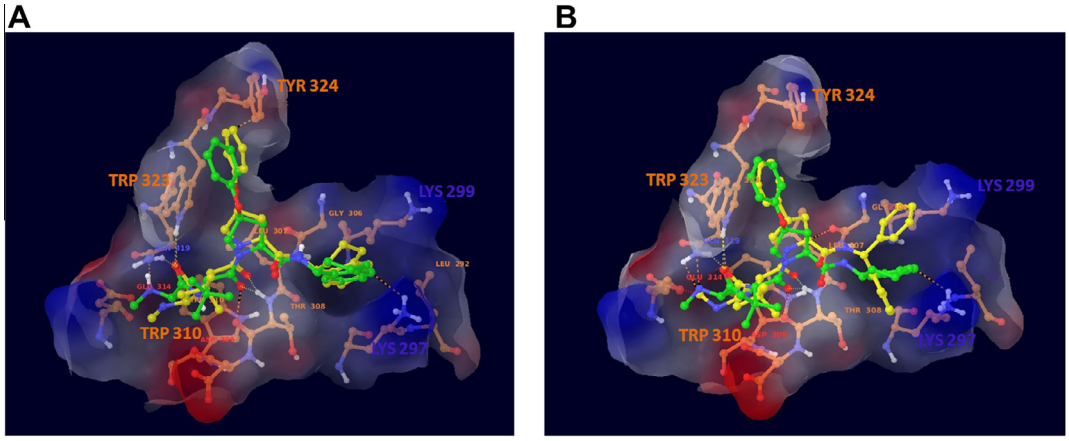

Figure 2. Binding poses of analogues **11b** (A) and **11c** (B) (both shown in yellow) in XIAP BIR3, overlapped with the peptidomimetic **11g** (shown in green).

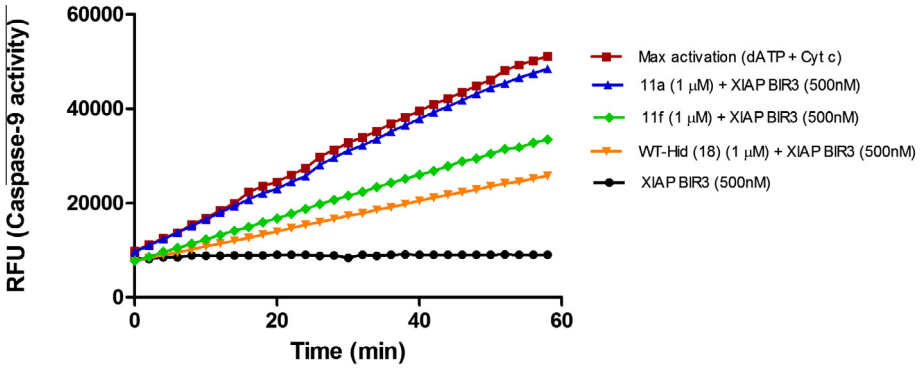

Figure 3. Caspase-9 activation data for (**11a**) and (**11f**) as examples of peptidomimetics in comparison to the WT-Hid (**18**).

and their tetrahydronaphthyl amide analogues (**11b**) and (**11d**) of % caspase-9 relief 87.6 ± 6.2 and 83.7 ± 7.1, respectively (Table 2); even though the in silico docking predicted the complete overlap of the indanyl ring with the tetrahydronaphthyl system. Furthermore, ligand (**10a**) demonstrated a 66.3 ± 8.4% caspase-9 activity recovery, which is equipotent to its 4-(*R*)-phenoxy proline analogue (**11e**) of 64.9 ± 9.3% caspase-9 activity recovery and slightly-but not significantly-stronger than its 4-(*S*)-phenyl proline analogue (**11f**) of 61.6 ± 8.6% caspase-9 activity recovery (Table 2). The rigidity of the tetrahydroisoquinoline ring fixed its phenyl ring part in an optimal position for the hydrophobic interaction with W323, although it does not project as deeply into the pocket as the 4-phenoxy substituted proline containing analogue (**11e**) (data not shown).

To validate the caspase-9 activity recovery assay, a series of Hid-derived N-terminal pentapeptides (**18**–**20**) of known binding affinity to XIAP BIR3[18] (Supplementary Table S4) were tested using the same assay, where Hid is the *Drosophila* functional analogue of human Smac/DIABLO.[29] It was gratifying to find that, the % caspase-9 relief recorded for those peptides matched their hierarchal binding affinity order (Supplementary Table S4 and Fig. S5). Consequently, the % caspase-9 activity recovery induced by our ligands can be used as a basis to compare their relative XIAP BIR3 binding affinities and also those of the Hid peptides. On this basis, the Smac/DIABLO-derived peptidomimetics (**11a**–**d**) prepared in this study and possessing % caspase-9 activity recovery range of ~93–83% are ~1.8-fold significantly stronger XIAP BIR3 inhibitors than the Hid peptides (**18**–**20**) of % caspase-9 activity recovery range ~43–55%, all tested at 1 μM concentration.

Consistent with the caspase-9 activity recovery assay, the % viability (MTT) assays showed moderate cytotoxicity of Smac/DIABLO-derived peptidomimetics (**11a**–**d**) at 100 μM concentration in the breast cancer MDA-MB-231 and MCF-7 cell lines, with a range of ~79–50% cell viability compared to untreated control (Table 2). In contrast, N-terminal Hid-derived peptides (**18**–**20**) exhibited no cytotoxicity against the same cell lines, when used at the same concentrations (data not shown).

Overall, the Smac/DIABLO-derived peptidomimetics (**11a**–**d**) showed significant improvement in the release/relief of caspase-9 inhibition caused by XIAP BIR3, compared to the N-terminal Hid-derived peptides (**18**–**20**). In addition, they also exhibited greater cytotoxicity against tumour cell lines, as assessed by MTT assays, in comparison to the Hid-derived peptides. This improvement is attributable to the SAR-based optimization and in silico aided design methods used to decide on the combinations of C-terminal capping groups and P3 residues of the sequences. These optimized alterations conferred better binding of (**11a**–**d**) to XIAP BIR3, and probably also improved their cell penetrability and resistance towards proteolytic cleavage, in comparison to Hid-derived peptides (**18**–**20**).

4. Conclusion

XIAP BIR3 inhibition by Smac/DIABLO-derived peptides can resensitize cancer cells to apoptosis. Accordingly, Smac/DIABLO-derived peptidomimetics were designed to improve both the XIAP BIR3 inhibition capacity and pro-apoptotic activity against intact cells. Based on the well-established SAR for Smac/DIABLO, 22

virtual ligands were designed, which were docked to XIAP BIR3 binding pocket. The ligands that exhibited best-fit and appropriate docking scores were synthesized by a novel SPPS strategy employing an Alkane sulfonamide 'Safety-Catch' resin. This approach afforded the rapid synthesis of the target peptidomimetic library and each of the member compounds was obtained in high % yield and purity. The use of the 'Safety-Catch' resin greatly facilitated the synthesis of the Smac/DIABLO-derived peptidomimetic library and has proved a novel alternative approach for the expedited synthesis of this class of compound that were previously only available through the much tedious classical solution methods.

These were then tested for their XIAP BIR3 inhibitory activity through a caspase-9 reactivation assay in presence of the apoptosome elements (Apaf-1, cytochrome c and dATP) with/without XIAP BIR3 domain. In general, candidates with 4-(*R*)-phenoxy substitution of the P3 pyrrolidine ring of the proline residue showed higher caspase-9 reactivation than the 4-(*S*)-phenyl analogues. This could be attributed to the deeper projection of phenoxy group into the hydrophobic pocket formed by residues W323 and Y324 (of XIAP BIR3) when compared to the corresponding phenyl analogues. This could reduce the inhibitory action of XIAP BIR3 and thus improve the caspase-9 reactivation induced by the 4-(*R*)-phenoxy analogues in comparison to the 4-(*S*)-phenyl analogues. Additionally, the peptidomimetic (**10a**) with Tic at P3 showed very similar caspase-9 reactivation to the 4-(*R*)-phenoxy analogues and in silico ligand superimposition demonstrated that both analogue types bound in a very similar manner. A study of the effectiveness of using differing aromatic ring C-terminal amide capping groups was also undertaken, since previous work has demonstrated that such groups are accommodated snugly into the hydrophobic channel formed by the K297 and K299 side chains of XIAP BIR3. As a general trend, it was found that the biphenyl amide capped compounds (**11a**) and (**11c**) exhibited higher caspase-9 reactivation than their tetrahydronaphthyl amide analogues (**11b**) and (**11d**), and both were stronger caspase-9 activators than their indolyl-3-methyl amide congeners (**11e**) and (**11f**). The biphenyl substituent is constrained and holds the phenyl rings in optimal positions for the hydrophobic interaction with K297 and K299 side chains.

Collectively, the Smac/DIABLO peptidomimetic (**11a**) with P1 *N*-methyl-L-alanine, P3 4-(*R*)-phenoxy proline and biphenyl amide capping at P4 exhibited the most potent caspase-9 activity restoration, with 93% caspase-9 relief being achieved at a concentration of 1 μM.

It was anticipated that these collective molecular properties would imbue these peptidomimetics with cell permeability and resistance to hydrolysis by proteases and so they were examined for their ability to cause loss of cell viability of a number of breast cancer cell lines. Compounds (**11a**–**d**) did indeed demonstrate moderate cytotoxicity against the breast cancer cell lines MDA-MB-231 and MCF-7, when used at a concentration of 100 μM. Whereas, in comparison, the Hid-derived N-terminal sequences (**18**–**20**), were inactive when tested against these cell lines. The relatively high dosing required to induce cytotoxicity, reflects the fact that Smac/DIABLO-derived peptidomimetics act as apoptosis resensitizers in cancer cells, rather than being apoptogenic agents, per se.

In final conclusion, the Smac/DIABLO-derived peptidomimetics represent an attractive class of compounds that can overcome tumour cell resistance to apoptosis, especially in cancer cells that over-express the anti-apoptotic XIAP protein.

Acknowledgments

This work was supported by the Dr. John King Foundation, through the provision of a Ph.D. studentship to Mohamed Elsawy. Many thanks for Dr. Rebecca Craig, School of Pharmacy, Queen's University of Belfast, for performing the ^{1}H NMR spectrometry analysis and to Christopher Hutchison, School of Pharmacy, Queen's University of Belfast, for the scientific discussion.

Supplementary data

Supplementary data associated with this article can be found, in the online version, at http://dx.doi.org/10.1016/j.bmc.2013.06.055.

References and notes

1. Ambrosini, G.; Adida, C.; Altieri, D. C. *Nat. Med.* **1997**, *3*, 917.
2. LaCasse, E. C.; Baird, S.; Korneluk, R. G.; MacKenzie, A. E. *Oncogene* **1998**, *17*, 3247.
3. Deveraux, Q. L.; Reed, J. C. *Genes Dev.* **1999**, *13*, 239.
4. Tamm, I.; Kornblau, S. M.; Segall, H.; Krajweski, S.; Welsh, K.; Kitada, S.; Scudiero, D. A.; Tudor, G.; Qui, Y. H.; Monks, A.; Andreeff, M.; Reed, J. C. *Clin. Cancer Res.* **2000**, *6*, 1796.
5. Du, C. Y.; Fang, M.; Li, Y. C.; Li, L.; Wang, X. D. *Cell* **2000**, *102*, 33.
6. Verhagen, A. M.; Ekert, P. G.; Pakusch, M.; Silke, J.; Connolly, L. M.; Reid, G. E.; Moritz, R. L.; Simpson, R. J.; Vaux, D. L. *Cell* **2000**, *102*, 43.
7. Ekert, P. G.; Silke, J.; Hawkins, C. J.; Verhagen, A. M.; Vaux, D. L. *J. Cell Biol.* **2001**, *152*, 483.
8. Srinivasula, S. M.; Hegde, R.; Saleh, A.; Datta, P.; Shiozaki, E.; Chai, J. J.; Lee, R. A.; Robbins, P. D.; Fernandes-Alnemri, T.; Shi, Y. G.; Alnemri, E. S. *Nature* **2001**, *410*, 112.
9. Krajewska, M.; Krajewska, S.; Banares, S.; Huang, X.; Turner, B.; Bubendorf, L.; Kallioniemi, O. P.; Shabaik, A.; Vitiello, A.; Peehl, D.; Gao, G. J.; Reed, J. C. *Clin. Cancer Res.* **2003**, *9*, 4914.
10. Salvesen, G. S.; Duckett, C. S. *Nat. Rev. Mol. Cell Biol.* **2002**, *3*, 401.
11. Srinivasula, S. M.; Datta, P.; Fan, X.-J.; Fernandes-Alnemri, T.; Huang, Z.; Alnemri, E. S. *J. Biol. Chem.* **2000**, *275*, 36152.
12. Chai, J.; Du, C.; Wu, J.-W.; Kyin, S.; Wang, X.; Shi, Y. *Nature* **2000**, *406*, 855.
13. Liu, Z.; Sun, C.; Olejniczak, E. T.; Meadows, R. P.; Betz, S. F.; Oost, T.; Herrmann, J.; Wu, J. C.; Fesik, S. W. *Nature* **2000**, *408*, 1004.
14. Wu, G.; Chai, J.; Suber, T. L.; Wu, J.-W.; Du, C.; Wang, X.; Shi, Y. *Nature* **2000**, *408*, 1008.
15. Fulda, S.; Wick, W.; Weller, M. *Nat. Med.* **2002**, *8*, 808.
16. Arnt, C. R.; Chiorean, M. V.; Heldebrant, M. P.; Gores, G. J.; Kaufmann, S. H. *J. Biol. Chem.* **2002**, *277*, 44236.
17. Yang, L.; Mashima, T.; Sato, S.; Mochizuki, M.; Sakamotor, H.; Yamori, T.; Oh-Hara, T.; Tsuruo, T. *Cancer Res.* **2003**, *63*, 831.
18. Oost, T. K.; Sun, C.; Armstrong, R. C.; Al-Assaad, A.; Betz, S. F.; Deckweth, T. L.; Ding, H.; Elmore, S. W.; Meadows, R. P.; Olejniczak, E. T.; Olesksijew, A.; Oltersdorf, T.; Rosenberg, S. H.; Shoemaker, A. R.; Tomaselli, K. J.; Zou, H.; Fesik, S. W. *J. Med. Chem.* **2004**, *47*, 4417.
19. Sun, H.; Nikolovska-Coleska, Z.; Chen, J.; Yang, C.-Y.; Tomita, Y.; Pan, H.; Yoshioka, Y.; Krajewski, K.; Roller, P. P.; Wang, S. *Bioorg. Med. Chem. Lett.* **2005**, *15*, 793.
20. Kipp, R. A.; Case, M. A.; Wist, A. D.; Cresson, C. M.; Carrell, M.; Griner, E.; Witta, A.; Albiniak, P. A.; Chai, J.; Shi, Y.; Semmelhack, M. F.; McLendo, G. L. *Biochemistry* **2002**, *41*, 7344.
21. Wist, A. D.; Gu, L.; Riedl, S. J.; Shi, Y.; McLendo, G. L. *Bioorg. Med. Chem.* **2007**, *15*, 2935.
22. Sun, H.; Nikolovska-Coleska, Z.; Yang, C. Y.; Xu, L.; Tomita, Y.; Krajewski, K.; Roller, P. P.; Wang, S. *J. Med. Chem.* **2004**, *47*, 4147.
23. Cai, Q.; Sun, H.; Peng, Y.; Lu, J.; Nikolovska-Coleska, Z.; McEachern, D.; Liu, L.; Qiu, S.; Yang, C.-Y.; Miller, R.; Yi, H.; Zhang, T.; Sun, D.; Kang, S.; Guo, M.; Leopol, L.; Yang, D.; Wang, S. *J. Med. Chem.* **2011**, *54*, 2714.
24. GLIDE 5.6. (2009) New York, NY, USA: Schrödinger, LLC.
25. New York, NY, USA:Schrodinger, LLC, 2010.
26. Backes, B. J.; Ellman, J. A. *J. Org. Chem.* **1999**, *64*, 2322.
27. Ding, Y.; Qin, C.; Guo, Z.; Niu, W.; Zhang, R.; Li, Y. *Chem. Biodivers.* **2007**, *4*, 2827.
28. Merkx, R.; Haren, M. J. V.; Rijkers, D. T. S.; Liskamp, R. M. J. *J. Org. Chem.* **2007**, *72*, 4574.
29. Vucic, D.; Kaiser, W. J.; Miller, L. K. *Mol. Cell. Biol.* **1998**, *18*, 3300.